Zinc Impurities in *d*-Wave Superconductors

Th. A. Maier and M. Jarrell

University of Cincinnati, Cincinnati, Ohio 45221
(Received 20 December 2001; published 26 July 2002)

We study the two-dimensional Hubbard model with nonmagnetic Zn impurities modeled by binary diagonal disorder using quantum Monte Carlo within the dynamical cluster approximation. With increasing Zn content we find a strong suppression of *d*-wave superconductivity and an enhancement of antiferromagnetic spin correlations. T_c vanishes linearly with Zn impurity concentration. The spin susceptibility changes from pseudogap to Curie-Weiss-like behavior indicating the existence of free magnetic moments in the Zn doped system. We interpret these results within the resonating-valence-bond picture.

Introduction.—Chemical substitution in high-T_c superconductors provides a powerful probe into the complex nature of both the superconducting and normal state of these materials. Experiments substituting different impurities for Cu show that nonmagnetic impurities (Zn, Al) are just as effective in suppressing superconductivity as magnetic dopants (Ni, Fe) [1]. Based on Anderson's theorem [2] these results are taken as strong evidence for an unconventional pairing state described by an anisotropic order parameter with nodes on the Fermi surface. Indeed, recently the characteristic fourfold symmetry of the $d_{x^2-y^2}$-wave order parameter was observed in the spatial variation of the local density of states near the Zn impurity using scanning tunneling microscopy [3].

Nuclear magnetic resonance experiments show that even a nonmagnetic impurity substituted for Cu induces an effective magnetic moment residing on the neighboring Cu sites [4]. In addition, the bulk susceptibility in impurity substituted underdoped cuprate superconductors shows Curie-Weiss-like behavior irrespective of the magnetic structure of the dopants [1]. This indicates the existence of free magnetic moments in the impurity doped CuO_2 planes. The formation of these moments with substitution of nonmagnetic impurities is explained to arise from breaking singlets [1,5] in an antiferromagnetically correlated host by removing Cu spins.

In this Letter we focus on the suppression of superconductivity by Zn impurities and the change of the bulk magnetic susceptibility to a Curie-Weiss-like behavior in underdoped systems. Despite a wide variety of theoretical studies addressing these issues, a complete understanding of the effects of Zn doping has not been achieved. These approaches are mostly based on the description of impurities embedded in a BCS host [6] or on generalizations of the Abrikosov-Gorkov equations for nonmagnetic impurities in unconventional superconductors using phenomenological pairing interactions [7]. In order to capture effects such as moment formation by substitution of nonmagnetic impurities, it seems necessary to describe correlations and the scattering from impurities on the same footing within a microscopic approach.

The most widely applied technique developed to describe disordered systems is the coherent potential approximation (CPA) [8]. The CPA shares the same microscopic definition [9] as its equivalent for correlated clean systems, the dynamical mean-field approximation (DMFA) [10]. Both approaches map the lattice system onto an effective impurity problem embedded in a host that represents the remaining degrees of freedom. This single-site approximation neglects interference effects of the scattering off different impurity sites (crossing diagrams) and correlation effects become purely local. Therefore, it inhibits a transition to a state described by a nonlocal (*d*-wave) order parameter and thus is not appropriate for our investigations here.

The dynamical cluster approximation (DCA) [9,11–13] systematically incorporates nonlocal corrections to the CPA/DMFA by mapping the lattice system onto an embedded periodic cluster of size N_c. For $N_c = 1$ the DCA is equivalent to the CPA/DMFA and by increasing the cluster size N_c the length scale of possible dynamical correlations can be gradually increased while the DCA solution remains in the thermodynamic limit. In the clean limit the DCA applied to the Hubbard model has been shown to describe the essential low energy physics of the cuprates [14–16]: It captures the antiferromagnetic phase near half filling and the transition to a superconducting phase with $d_{x^2-y^2}$-wave order parameter at finite doping. In the normal state it exhibits non-Fermi liquid behavior in the form of a pseudogap in the density of states and a suppression of spin excitations at low temperatures in the underdoped regime.

In this Letter we study the two-dimensional (2D) Hubbard model including a potential scattering term according to the chemistry of Zn impurities using the DCA for a cluster size $N_c = 4$. We show that potential scattering by Zn impurities strongly suppresses superconductivity as well as spin fluctuations and changes the magnetic susceptibility to a Curie-Weiss-like temperature dependence in the underdoped region.

Formalism.—The correlated electrons in a CuO_2 plane doped with Zn impurities are described by the 2D Hubbard model with diagonal disorder

$$H = -t \sum_{\langle ij\rangle,\sigma} c_{i\sigma}^{\dagger} c_{j\sigma} + U \sum_{i} n_{i\uparrow} n_{i\downarrow} + \sum_{i\sigma} \epsilon_i n_{i\sigma}, \quad (1)$$

where we used standard notation. The disorder induced by the Zn sites occurs in the local orbital energies ϵ_i which are independent quenched random variables distributed according to some specified distribution $P(\epsilon_i, \ldots, \epsilon_N) = \prod_{i=1}^{N} P(\epsilon_i)$, where N is the number of lattice sites. For a concentration x of Zn impurities we use the binary alloy distribution

$$P(\epsilon_i) = x\delta(\epsilon_i + V/2) + (1-x)\delta(\epsilon_i - V/2), \quad (2)$$

where V is the energy difference between the Cu and Zn $3d$ orbitals. For simplicity we use site-independent values for the hopping integral t and the Coulomb repulsion U.

The microscopic derivation of the DCA algorithm was discussed in detail for correlated systems in [12,16] and for disordered systems in [9]. The DCA has a simple physical interpretation for systems where the intersite correlations have only short spatial range. The corresponding self-energy may then be calculated on a coarse grid of $N_c = L_c^D$ selected $\mathbf{K}$ points only, where L_c is the linear dimension of the cluster of $\mathbf{K}$ points. Knowledge of the momentum dependence on a finer grid may be discarded to reduce the complexity of the problem. To this end the first Brillouin zone is divided into N_c cells of size $(2\pi/L_c)^D$ around the cluster momenta $\mathbf{K}$. The propagators used to form the self-energy are coarse grained or averaged over the momenta $\mathbf{K} + \tilde{\mathbf{k}}$ surrounding the cluster momentum $\mathbf{K}$:

$$\bar{G}(\mathbf{K}, i\omega_n) = \frac{N_c}{N} \sum_{\tilde{\mathbf{k}}} G(\mathbf{K} + \tilde{\mathbf{k}}, i\omega_n)$$
$$= \frac{N_c}{N} \sum_{\tilde{\mathbf{k}}} \frac{1}{i\omega_n - \epsilon_{\mathbf{K}+\tilde{\mathbf{k}}} - \Sigma(\mathbf{K}, i\omega_n)}. \quad (3)$$

In Eq. (3) we make use of the fact that the approximation of the lattice self-energy $\Sigma(\mathbf{k})$ by the cluster self-energy $\Sigma(\mathbf{K})$ optimizes the free energy [12,13]. $\Sigma(\mathbf{K})$ summarizes the single-particle effects of the interaction term (second term) and the disorder term (third term) of the Hamiltonian, Eq. (1). The dispersion $\epsilon_{\mathbf{K}+\tilde{\mathbf{k}}}$ denotes the spectrum of the kinetic part (first term) of Eq. (1). In order to avoid overcounting of self-energy diagrams on the cluster, the cluster excluded propagator

$$\mathcal{G}(\mathbf{K})^{-1} = \bar{G}(\mathbf{K})^{-1} + \Sigma(\mathbf{K}) \quad (4)$$

is used as the bare propagator for the cluster problem. To diagonalize the disorder part it is convenient to perform a Fourier transform to cluster real space $\mathcal{G}_{ij} = 1/N_c \sum_{\mathbf{K}} e^{i\mathbf{K}\cdot(\mathbf{X}_i - \mathbf{X}_j)} \mathcal{G}(\mathbf{K})$, where the disorder is diagonal. The inverse bare cluster propagator for a particular disorder configuration $\{\epsilon_i\}$ is then given by

$$[\mathcal{G}_{\epsilon_1,\ldots,\epsilon_N}^{-1}]_{ij} = [\mathcal{G}^{-1}]_{ij} - \epsilon_i \delta_{ij}, \quad (5)$$

and is used to initialize a quantum Monte Carlo (QMC) simulation to calculate the effects of the Coulomb inter-

action U. The QMC result for the cluster Green function $G_{\epsilon_1,\ldots,\epsilon_N,ij}^c = G_{ij}^c[U, \mathcal{G}_{\epsilon_1,\ldots,\epsilon_N,ij}]$ thus depends on the particular disorder configuration $\{\epsilon_i\}$. The disorder averaged cluster Green function is then obtained from the individual results by

$$G_{ij}^c = \langle G_{\epsilon_1,\ldots,\epsilon_N,ij}^c \rangle, \quad (6)$$

where the average $\{\cdots\} = \int \prod_{i=1}^{N} d\epsilon_i P(\epsilon_i)(\cdots)$ is to be taken for a system of N_c sites. Note that in principle QMC calculations for all possible disorder configurations $\{\epsilon_i\}$ have to be carried through. However, contributions from configurations with m Zn impurities on the cluster ($m \leq N_c$) are weighted by a factor of $x^m (1-x)^{(N_c-m)}$ to the integral Eq. (6). Therefore it seems reasonable for small concentrations $x < 1/N_c$ to consider only those configurations with none or only a single Zn impurity on the cluster and to neglect configurations with more than one Zn impurity. Then the disorder averaged cluster Green function G_{ij}^c is obtained as a weighted sum from the two configurations as

$$G_{ij}^c = x N_c G_{1,ij}^c + (1 - x N_c) G_{0,ij}^c, \quad (7)$$

where $G_{1/0,ij}^c$ denotes the QMC result for the cluster Green function for the configuration with one or zero Zn impurities on the cluster, respectively. The prefactors follow with $(1-x)^{N_c} \approx 1 - x N_c$, $x N_c (1-x)^{N_c-1} \approx x N_c$ for $x \ll 1$ in linear approximation in the impurity concentration x. The disorder averaged cluster Green function G_{ij}^c is then transformed back to cluster reciprocal space to calculate a new estimate of the cluster self-energy

$$\Sigma(\mathbf{K}) = \mathcal{G}(\mathbf{K})^{-1} - G^c(\mathbf{K})^{-1}, \quad (8)$$

which is then used to repeat the steps starting from Eq. (3) until convergence is reached.

Results.—We study the superconducting instability and magnetic properties of the Hamiltonian Eq. (1) in the intermediate coupling regime at 5% hole doping ($n = 0.95$) for different Zn impurity concentrations x. We perform calculations for $N_c = 4$, the smallest cluster size that allows for a transition to a $d_{x^2-y^2}$-wave superconducting state while preserving the lattice translational and point group symmetries. We set the hopping integral $t = 0.25$ eV and the Coulomb repulsion $U = W = 2$ eV, where $W = 8t$ is the bandwidth of the noninteracting system. We choose $V = 5$ eV $> W + U$ to simulate the nonmagnetic closed shell (d^{10}) configuration of the impurity site.

We searched for superconductivity with *s*-wave, extended *s*-wave, *p*-, and *d*-wave order parameters. As we found for the clean system ($x = 0$) [14,16], only the $d_{x^2-y^2}$-wave pair-field susceptibility for zero center of mass momentum diverges at low temperatures. Please note that the finite transition temperatures we find for the 2D system arise from the residual mean-field character of the DCA for finite cluster sizes N_c. Preliminary results indicate that with increasing cluster size this transition

can be stabilized at finite temperatures if an interplanar coupling between the 2D Hubbard planes is added [16]. Figure 1 illustrates the inverse pair-field susceptibility P_d^{-1} as a function of temperature T for the impurity concentrations $x = 0.00$ (circles), $x = 0.05$ (squares), and $x = 0.10$ (diamonds).

The corresponding critical temperature T_c is then calculated by extrapolating $P_d^{-1}(T)$ to zero using the function $P_d^{-1} \propto (T - T_c)^{\gamma}$ (represented by the solid lines in Fig. 1). T_c is rapidly suppressed, and the critical exponent γ increases, with increasing Zn content x. Consistent with experiments [1] this falloff of T_c is linear in x resulting in a critical impurity concentration $x_c \approx 0.10$, beyond which the instability to the superconducting phase disappears. Compared to experiments ($x_c \lesssim 0.05$) our calculation predicts a result about twice as high for the critical doping. However, considering the simplified description of the problem using a 2D Hubbard model with the complexity of the Zn impurities reduced to a model of diagonal disorder, we expect agreement only on a qualitative level.

In order to study the correlation between the suppression of superconductivity and possible moment formation by Zn substitution we study the bulk [$\mathbf{q} = (0, 0)$] and the antiferromagnetic [$\mathbf{q} = (\pi, \pi)$] spin susceptibilities. Figure 2 shows the bulk magnetic susceptibility $\chi(T)$ as a function of temperature for the same impurity concentrations x used in Fig. 1.

As we demonstrated in [14] and similarly seen in finite size simulations [17], the clean system exhibits an anomaly in $\chi(T)$ at a characteristic temperature $T^{\star}$, below which spin excitations are suppressed and $\chi(T)$ falls with decreasing temperature. $T^{\star}$ thus marks the onset of singlet formation due to strong short-ranged antiferromagnetic spin correlations. In agreement with experiments [1], the substitution of impurities leads to a dramatic change of the low temperature behavior of the magnetic spin susceptibility. Despite the nonmagnetic nature of the impurity scattering term in our simulation, $\chi(T)$ displays an upturn at low temperatures as x is increased. Moreover at $x = 0.10$, $\chi(T)$ shows Curie-Weiss-like behavior; i.e., it can be fit by the function $\chi(T) = \chi_0 - \chi_1 T + C/(T - \Theta)$, with $\Theta \approx 0$. This clearly indicates the formation of free magnetic moments due to the breaking of singlet bonds by the substitution of nonmagnetic impurities. As illustrated in the inset in Fig. 1, these magnetic moments are located on the nearest-neighbor sites (nn 1 and nn 2) of the Zn impurity. With decreasing temperature, $T\chi_{ii}$ on these sites seems to extrapolate to a finite value at $T = 0$, indicating the absence of Kondo screening. Moreover, it is interesting to note that the magnetic moment on the next nearest-neighbor (nnn) site is smaller than the magnetic moment on the pure cluster.

The inverse antiferromagnetic spin susceptibility $\chi_{AF}(T)$ for the same parameter set as in Fig. 2 is illustrated in Fig. 3. For the clean system ($x = 0$) 5% hole doping marks the critical doping, beyond which no transition to an antiferromagnetic state can be found [14]. As can be seen from the extrapolation of the circles in Fig. 3 the corresponding Néel temperature $T_N = 0$. As the concentration of impurities is increased we notice that for $T \gtrsim 0.05$ χ_{AF} decreases with x. However at lower temperatures ($T \lesssim 0.05$) χ_{AF}^{-1} for finite impurity concentration x falls below the curve of the clean system and eventually goes through zero indicating a transition to the antiferromagnetic state. Therefore it can be inferred that a finite concentration of impurities, i.e., spin vacancies, acts to enhance antiferromagnetic spin correlations.
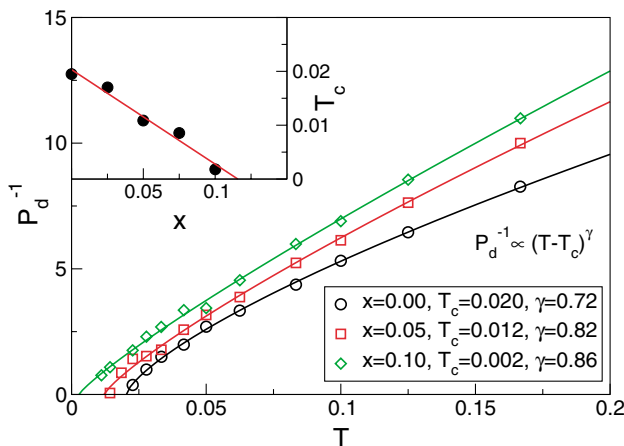

FIG. 1 (color online). The inverse pair-field susceptibility versus temperature when $N_c = 4$, $U = W = 2$ eV, $V = 5$ eV at 5% doping for impurity concentrations $x = 0.00$ (circles), $x = 0.05$ (squares), and $x = 0.10$ (diamonds). The solid lines represent fits to the function $P_d^{-1} \propto (T - T_c)^{\gamma}$. Inset: Critical temperature T_c as a function of impurity concentration x.
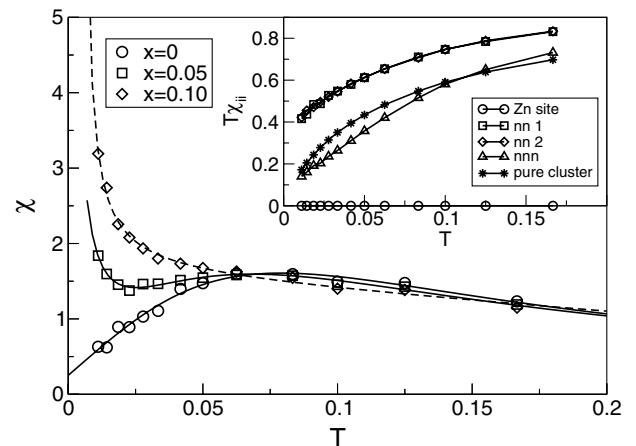

FIG. 2. The bulk magnetic susceptibility versus temperature when $N_c = 4$, $U = W = 2$ eV, $V = 5$ eV at 5% doping for impurity concentrations $x = 0$ (circles), $x = 0.05$ (squares), and $x = 0.10$ (diamonds). The solid lines are guides to the eye. The dashed line represents a fit to the function $\chi(T) = \chi_0 - \chi_1 T + C/(T - \Theta)$. Inset: Time averaged local magnetic moment on the Zn site, on its nearest (nn 1, nn 2) and next nearest (nnn) neighbors and on the pure cluster.
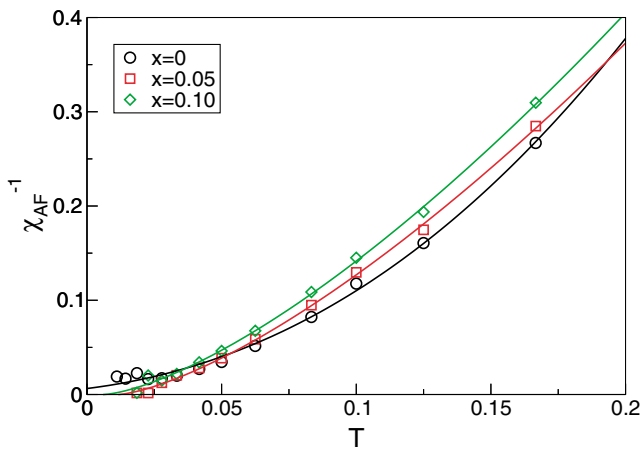
FIG. 3 (color online). The inverse antiferromagnetic $[\mathbf{q} = (\pi, \pi)]$ spin susceptibility versus temperature when $N_c = 4$, $U = W = 2$ eV, $V = 5$ eV at 5% doping for impurity concentrations $x = 0$ (circles), $x = 0.05$ (squares), and $x = 0.10$ (diamonds). The solid lines represent fits to the function $\chi_{AF}^{-1} \propto (T - T_N)^\gamma$.

It is important to note that recent NMR measurements on $YBa_2Cu_3O_{6.7}$ [18] show a similar enhancement of antiferromagnetic spin correlations around Zn impurities at low temperatures.

Similar results were also obtained in [19,20] where an antiferromagnetic Heisenberg model with a spin vacancy was studied. In the latter report, the enhancement of antiferromagnetic spin correlations was ascribed to *pruning* of singlets by the nonmagnetic impurity in a resonating-valence-bond (RVB) picture. In the RVB picture, the short-ranged order in the doped model is described as a collection of nearest-neighbor singlet bonds which fluctuate as a function of time and space. When a Zn impurity is introduced into the system, the singlet fluctuations on adjacent sites are suppressed since these sites now have one less neighbor to form short-ranged bonds with. The suppression of singlet fluctuations on the sites adjacent to the Zn dopant thus enhances antiferromagnetic spin correlations on these sites.

We find further evidence of the suppression of beyond mean-field spin fluctuations by Zn impurities in the decrease of the antiferromagnetic critical exponent γ towards the mean-field result of one with increasing impurity content x. Concomitant with this behavior the corresponding exponent γ for the pair-field susceptibility (cf. Fig. 1) increases towards one. From this observation we conclude that the suppression of superconductivity in Zn doped systems originates in the suppression of beyond mean-field spin fluctuations that mediate pairing.

Summary.—In this Letter we have used the 2D Hubbard model with binary diagonal disorder to study the effects of nonmagnetic (Zn) impurities on high-temperature superconductivity. We find that Zn impurities strongly suppress superconductivity. As evidenced by the increasing mean-field character of the pair-field and antiferromagnetic susceptibilities with Zn substitution, spin fluctuations beyond mean field that mediate pairing get suppressed. Consistent with experiments, T_c decreases linearly with impurity concentration. With increasing Zn content we further find a change of the magnetic susceptibility to Curie-Weiss-like behavior originating in the existence of free magnetic moments, which are located in the vicinity of the Zn impurity.

Our results can be understood within the RVB picture. The nonmagnetic impurities break local singlets and thus generate unpaired spins. A concomitant suppression of singlet fluctuations that mediate pairing results from the pruning of RVB states [20]. Consequently, superconductivity gets strongly suppressed with increasing Zn content.

[1] G. Xiao *et al.*, Phys. Rev. B **42**, 8752 (1990).
[2] P. W. Anderson, J. Phys. Chem. Solids **11**, 26 (1995).
[3] S. H. Pan *et al.*, Nature (London) **403**, 746 (2000).
[4] H. Alloul *et al.*, Phys. Rev. Lett. **67**, 3140 (1991); A. V. Mahajan *et al.*, Phys. Rev. Lett. **72**, 3100 (1994).
[5] A. M. Finkelstein *et al.*, Physica (Amsterdam) **168C**, 370 (1990).
[6] T. Xiang and J. M. Wheatley, Phys. Rev. B **51**, 11 721 (1995); G. Harań and A. D. S. Nagi, Phys. Rev. B **58**, 12 441 (1998).
[7] R. J. Radtke *et al.*, Phys. Rev. B **48**, 653 (1993); S. Haas *et al.*, Phys. Rev. B **56**, 5108 (1997).
[8] D. W. Taylor, Phys. Rev. **156**, 1017 (1967); P. Soven, Phys. Rev. **156**, 809 (1967); P. L. Leath and B. Goodman, Phys. Rev. **148**, 968 (1966).
[9] M. Jarrell and H. R. Krishnamurthy, Phys. Rev. B, **63**, 125102 (2001).
[10] W. Metzner and D. Vollhardt, Phys. Rev. Lett. **62**, 324 (1989); E. Müller-Hartmann, Z. Phys. B **74**, 507–512 (1989); T. Pruschke *et al.*, Adv. Phys. **42**, 187 (1995); A. Georges *et al.*, Rev. Mod. Phys. **68**, 13 (1996).
[11] M. H. Hettler *et al.*, Phys. Rev. B **58**, R7475 (1998).
[12] M. H. Hettler *et al.*, Phys. Rev. B **61**, 12 739 (2000).
[13] Th. Maier *et al.*, Eur. Phys. J. B **13**, 613 (2000).
[14] M. Jarrell *et al.*, Europhys. Lett. **56**, 563 (2001).
[15] Th. Maier *et al.*, Phys. Rev. Lett. **85**, 1524 (2000).
[16] M. Jarrell *et al.*, Phys. Rev. B **64**, 195130 (2001).
[17] A. Moreo, Phys. Rev. B **48**, 3380 (1993).
[18] M.-J. Julien *et al.*, Phys. Rev. Lett. **84**, 3422 (2000).
[19] N. Bulut *et al.*, Phys. Rev. Lett. **62**, 2192 (1989).
[20] G. B. Martins *et al.*, Phys. Rev. Lett. **78**, 3563 (1997).